INVITED PAPER Special Section on Silicon Photonics Technologies and Their Applications

The Transmission Properties of One-Bus Two-Ring Devices

Landobasa Y.M.A.L. TOBING[†a)], Pieter DUMON[††], Roel BAETS[††], Desmond. C.S. LIM[†], *and* Mee-Koy CHIN[†], *Nonmembers*

SUMMARY We propose and demonstrate a simple one-bus two-ring configuration where the two rings are mutually coupled that has advantages over the one-ring structure. Unlike a one cavity system, it can exhibit near critically-coupled transmission with a broader range of loss. It can also significantly enhance the cavity finesse by simply making the second ring twice the size of the bus-coupled one, with the enhancement proportional to the intensity buildup in the second ring.

key words: *microring resonator, critical coupling, silicon on insulator, integrated optics*

1. Introduction

Microring resonators are compact, low-loss devices that can generate high-Q resonances useful for many functions such as modulators [1], switching [2] and sensing [3], [4]. In the simplest configuration, one microring is coupled evanescently with one waveguide bus through which light is transmitted. Under certain coupling condition [5], [6] the light coupled into the cavity can be totally absorbed, giving rise to a resonant zero in the transmission spectrum. The device can then serve as an efficient optical switch or sensor, if the cavity loss or coupling coefficient can be tuned or affected by the environment. However, it is not easy to achieve critical coupling by matching the coupling coefficient with the round-trip loss because the later is unknown and both are dependent on fabrication condition as well as the device geometry. It is therefore desirable to have a way to realize critical coupling that is less sensitive to cavity geometry and loss.

In this paper, we propose and demonstrate a simple modification of the one-ring one-bus (1R1B) geometry that can exhibit near critical-coupling transmission with a broader range of loss. The new configuration consists of two mutually coupled rings coupled to one waveguide bus, as shown in Fig. 1(a). The two-ring geometry provides two possible optical pathways, shown as P1 and P2 in the figure. By virtue of the interference between these optical pathways it is possible to realize significant finesse enhancement compared with that based on one ring. The finesse enhancement in general amplifies the effect of loss in any cavity geometry, thereby relaxing the critical coupling condition in the coupled rings. In particular, the finesse is maximum when ring 2 is twice the size of ring 1. The narrow linewidth is useful for many high-Q applications such as bio-chemical sensing, switching, and optical buffer. The devices are experimentally demonstrated in low-finesse microrings fabricated in Silicon-on-Insulator (SOI) wafer using Deep-UV (DUV) lithography [7], [8], and the results are in good agreement with theory. In the following we first discuss the theory and then compare it with the experimental results.

Manuscript received July 6, 2007.

[†]The authors are with Nanyang Technological University, Singapore.

[††]The authors are with Ghent University, Belgium.

a) E-mail: LAND0001@ntu.edu.sg

DOI: 10.1093/ietele/e91–c.2.167

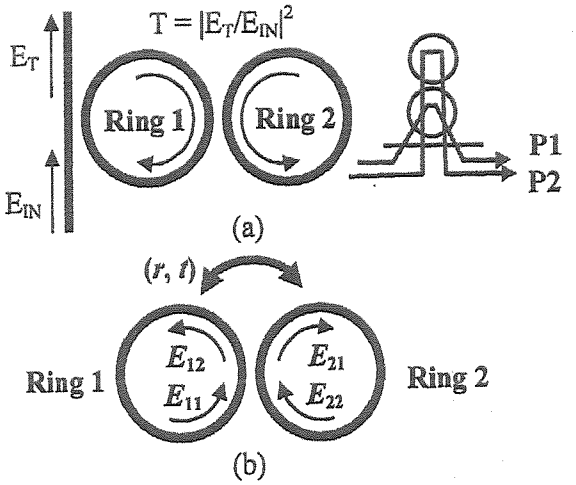

Fig. 1 (a) The schematic of two ring coupled to one waveguide bus. The excited optical pathways are shown in the right inset. (b) The fields and the coupling coefficients for the bare two-ring.

2. Theory

In the bare double-ring structure shown in Fig. 1(b), the resonance modes from each ring interact and give rise to resonance splitting, as is well known in coupled-resonator systems. The coupling of fields between the two rings is assumed to be phase-matched and lossless, as given by

$$\begin{pmatrix} E_{12} \\ E_{21} \end{pmatrix} = \begin{pmatrix} r & it \\ it & r \end{pmatrix} \begin{pmatrix} E_{11} \\ E_{22} \end{pmatrix},$$

where r and t are the reflection and transmission coupling coefficients and $|r|^2 + |t|^2 = 1$. In the lossless and steady-state situation, the fields obey continuity condition, and it is easy to show that

$$\tau_{21} = \frac{E_{12}}{E_{11}} = \exp(i\delta_1) = \frac{r - \exp(-i\delta_2)}{1 - r\exp(-i\delta_2)},$$
$$\tau_{12} = \frac{E_{21}}{E_{22}} = \exp(i\delta_2) = \frac{r - \exp(-i\delta_1)}{1 - r\exp(-i\delta_1)}, \quad (1)$$

where τ_{ij} is the effective phase shift in the field in ring i induced by coupling with ring j, and δ_j is the round-trip phase (or normalized frequency) in ring j, $\delta_j = \omega\tilde{T}_j = \omega n_{\text{eff}}^{(j)} L_j/c$, where $\tilde{T}_j$ and L_j are respectively the round trip time and cavity length of ring j. Equation (1) can be reduced to the following characteristic relation between δ_1 and δ_2 for arbitrary ring sizes:

$$\cos(\gamma + 1)\delta_1/2 = r\cos(\gamma - 1)\delta_1/2, \tag{2}$$

where $\gamma = \delta_2/\delta_1$. Equation (2) determines the resonance frequencies for arbitrary value of γ. We consider the case where γ varies from 1 to 2. When $\gamma = 1$, the rings are identical, and the resonance is split symmetrically about $\delta_1 = 2\,\text{m}\pi$ according to

$$\delta_1 = \pm\cos^{-1}(r) = \pm\sin^{-1}(t), \tag{3}$$

which clearly shows that the stronger the coupling between the rings the wider is the splitting. When γ=2, Eq. (2) has three solutions corresponding to three resonances. Two of these arise from a symmetric splitting around $\delta_1 = 2\,\text{m}\pi$ given by $\delta_1 = \pm\cos^{-1}[(1 + r)/2]$. Note that this splitting is smaller than that for γ=1. The third resonance is narrower and occurs whenever δ_1/π is odd.

To excite these resonances the two rings are coupled to a single bus waveguide (see Fig. 1(a)). The transmission is expected to be similar to that of a single ring coupled to one bus waveguide, but "loaded" with another ring (ring 2). The through transmission is thus given by [9]

$$T = \left|\frac{E_T}{E_{IN}}\right|^2 = \left|\frac{r_1 - a_1\tau_{21}\exp(-i\delta_1)}{1 - a_1 r_1\tau_{21}\exp(-i\delta_1)}\right|^2 \tag{4}$$

where r_1 is the coupling coefficient between ring 1 and the waveguide bus, $a_j = \exp(-\alpha L_j/2)$ is the round-trip amplitude which accounts for the loss in the jth ring, and τ_{21} is the loading factor similar to Eq. (1) but in the presence of loss is given by $\tau_{21} = \frac{(r - a_2\exp(-i\delta_2))}{(1 - a_2 r\exp(-i\delta_2))}$. Writing $\tau_{21} = |\tau_{21}|\exp(-i\delta_{\text{load}})$, Eq. (4) can be recast as

$$T = \left|(r_1 - \tilde{a}_1\exp(-i\delta))/(1 - \tilde{a}_1 r_1\exp(-i\delta))\right|^2 \tag{5}$$

where $\tilde{a}_1 = a_1|\tau_{21}|$ and $\delta = \delta_1 - \delta_{\text{load}}$ is the modified round trip phase:

$$\delta = \delta_1 - \left[\tan^{-1}\left(\frac{a_2\sin\delta_2}{r - a_2\cos\delta_2}\right) - \tan^{-1}\left(\frac{a_2 r\sin\delta_2}{1 - a_2 r\cos\delta_2}\right)\right] \tag{6}$$

which is the phase difference between the two optical pathways shown in Fig. 1(a).

The interference of the two pathways determines the features of the transmission spectra. The transmission is minimum when δ=0 or even multiples of π. Some examples are shown in Fig. 2 for γ values between 1 and 2, assuming $a_1 = 0.96$, $r_1 = 0.8$, and $r = 0.92$. These values are chosen to match with the experimental data to be presented later. When the rings are identical, the splitting is symmetrical. As γ deviates from 1 the resonance is split asymmetrically into a broad and a narrow resonance. The broad resonance is associated with ring 1 and the narrow resonance with ring 2. This is because ring 2 is isolated from the waveguide bus, hence the light needs to resonate in ring 1 before exiting the structure, and so the overall cavity lifetime is longer corresponding to a narrower linewidth. For the same reason, the transmission at the narrow resonance is inevitably lower. For $\gamma = 1.5$, there are two alternating patterns, one consisting of two split resonances, and the other two narrow and one broad resonance. This occurs because of the Vernier effect where, for $\gamma = 1.5$, the resonances for both rings coincide when δ_1/π is even-valued.

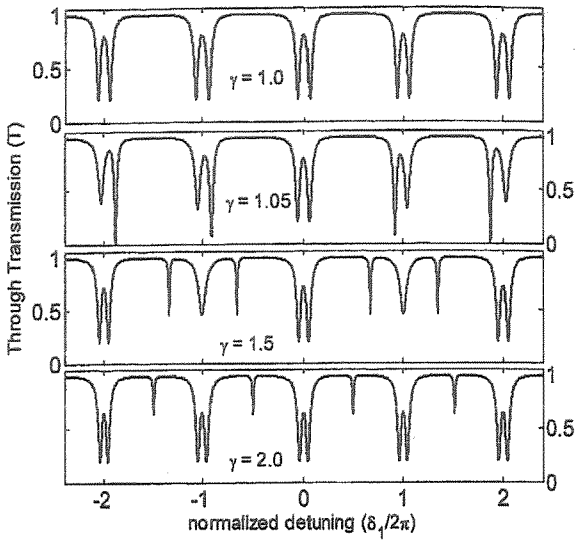

Fig. 2 The through transmission T for different values of γ. The loss is set to 0.96, the coupling coefficients are $r = 0.92$ and $r_1 = 0.8$. These values are chosen to match with the experimental data of Fig. 6.

In general, as γ increases the separation between the split resonances increases, and the linewith of the narrow resonance decreases and become more symmetrical. When γ=2, there are three resonances. The broad resonance associated with ring 1 is symmetrically split around $\delta_1 = 2\,\text{m}\pi$ in a way similar to the case γ=1, except that the field intensity is distributed inversely proportional to the ring size. The third, narrow resonance is located at an odd value of δ_1/π (and even. value of δ_2/π) and thus is centered exactly between two adjacent broad resonances and the lineshape is symmetrical. In this case, ring 1 is said to be "anti-resonant" while ring 2 is resonant, hence light is trapped more strongly in ring 2, giving rise to the narrowest linewidth. The factor by which the linewidth is reduced compared to that of the single-ring configuration is proportional to the intensity buildup factor in ring 2 relative to the intensity in ring 1, which is given by

$$B_{21} = (1 - r^2)/(1 - a_2 r)^2 \tag{7}$$

It can be shown that B_{21} is the maximum slope of the phase perturbation $\delta_{\text{load}} = \arg(\tau_{12})$ given by Eq. (1). This finesse enhancement factor can be quite large if ring 2 has very low loss and low coupling coefficient (high r).

The analytical results have been verified by Finite Difference Time Domain (FDTD) simulations of the field dis-

tribution. As shown in Fig. 3, in the case of $\gamma = 1$, the field is equally confined in both rings, while for $\gamma = 2$, the field is approximately twice larger in ring 1 than in ring 2 for the broad resonance, and is dominantly confined in ring 2 for the narrow resonance.

Similar to the one-ring case, the critical coupling condition is given by $r_1 = \tilde{a}_1$, and is a function of r_1 and r for a given γ and round-trip loss (a_1). Figure 4 shows, for the case $\gamma = 2$, the transmission at the narrow resonance as a function of r, for various given values of r_1 and with the loss kept constant (in this case, $a_1 = 0.999$). It can be seen that critical coupling can be satisfied by various combinations of (r_1, r), where r is higher if r_1 is lower, and vice versa. This means that one can achieve critical coupling for any arbitrary cavity loss by tuning r_1 and r, which gives the two-ring device greater flexibility in achieving critical coupling than is possible with the one-ring geometry. For example, if $r_1 < a_1$, then critical coupling is difficult for the one-ring device as it is not easy to increase loss (reduce a_1). On the other hand, for the two-ring structure, ring 2 can be made with higher finesse (higher r) to enhance the effective loss ($\tilde{a}_1$) so as to match r_1 and achieve critical coupling. Furthermore, we can see that, although the transmission is quite sensitive to r, one can still achieve a reasonably good extinction (say, −10 dB) over quite a broad range of r if the round-trip loss is very low ($a_1 = 0.999$). This cannot be obtained by one ring alone.

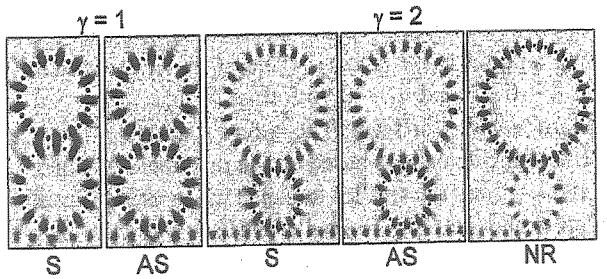

Fig. 3 The field distribution for $\gamma = 1$ and $\gamma = 2$ as calculated using FDTD. Note that the two symmetric resonances have a symmetric (S) and an anti-symmetric (AS) transverse field profile at the coupling point. The NR stands for near critical coupling corresponding to the narrow resonance for $\gamma = 2$.

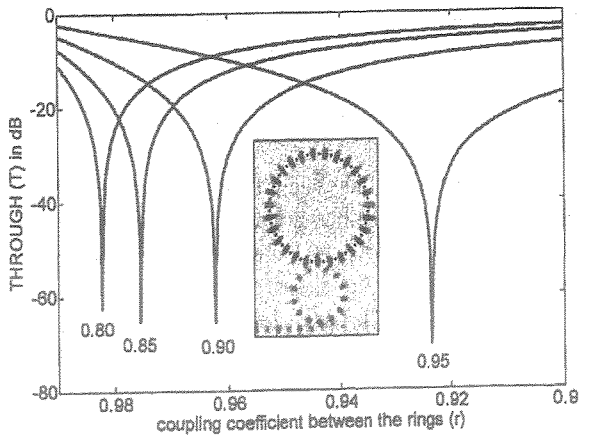

Fig. 4 The critical coupling condition for different values of r_1 as a function of the inter-ring coupling coefficient r. The inset shows the field distribution of the narrow resonance.

3. Experimental Result

The device is fabricated in IMEC under the SOI e-PIXnet platform using CMOS deep-UV process [7], [8]. The SOI consists of 220 nm Silicon on a 2 μm oxide cladding layer. The nominal waveguide width is 440 nm and the nominal gap separation between the waveguide and the ring is 167 nm. However, in the DUV lithography process, the exposure dose is incrementally stepped up from the left to the right of the 8" wafer such that the gap width (waveguide width) increases (decreases) from left to right of the wafer. These variations imply that different devices on the wafer will have different coupling coefficients, and hence one can study the device behavior with various coupling coefficients of interest. Two devices with different values of γ are shown in Fig. 5, where the resonators have radii of R_1 and R_2 and are coupled with each other and with the bus via racetracks of lengths L_1 and L_2 which determine the coupling coefficients. These parameters are summarized in Table 1 for four different γ values.

Two sets of devices are tested in order to have a wider range of values for the loss parameter a: Set A has an air cladding on top while Set B has an oxide cladding deposited on top by plasma-enhanced chemical vapor deposition. For Set B we can expect a much lower sidewall scattering loss as well as stronger coupling because of the smaller index contrast.

For measurement a second-order grating is integrated with the device to facilitate fiber coupling, in which the fiber is butt-coupled to the grating at 10° off vertical. The coupling efficiency has a Gaussian spectral dependence with a bandwidth of about 30 nm. The device is excited with a broadband source with wavelength ranging from 1.41 μm to 1.62 μm. The measured transmission is normalized by the input spectrum and adjusted for the grating envelop and polarization dependence. The final spectra are shown in Figs. 6 and 7, respectively, for the two sets of devices. Note that

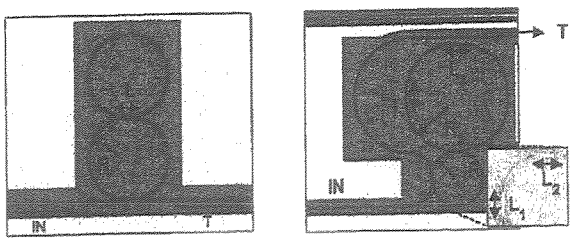

Fig. 5 The fabricated mutually coupled rings.

Table 1 The elongation parameter for the last 3 devices is $L_3 = L_1$.

R_1	R_2	L_1	L_2	Γ
15	15.0	2.0	2.0	~1.000
15	15.8	5.4	3.0	~1.045
15	23.8	5.4	3.0	~1.497
15	32.7	5.4	3.0	~2.000

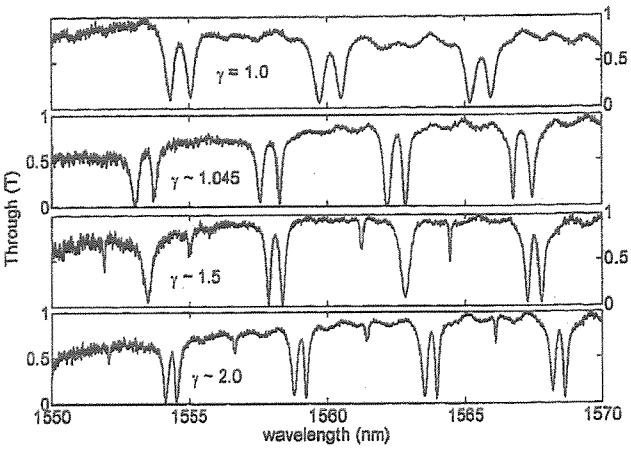

Fig. 6 The through spectra for the devices without upper oxide cladding: for values of γ in Table 1.

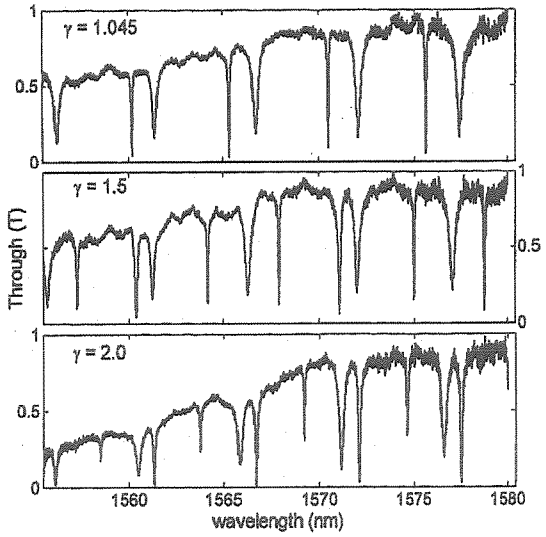

Fig. 7 The transmission spectra for devices with upper oxide cladding.

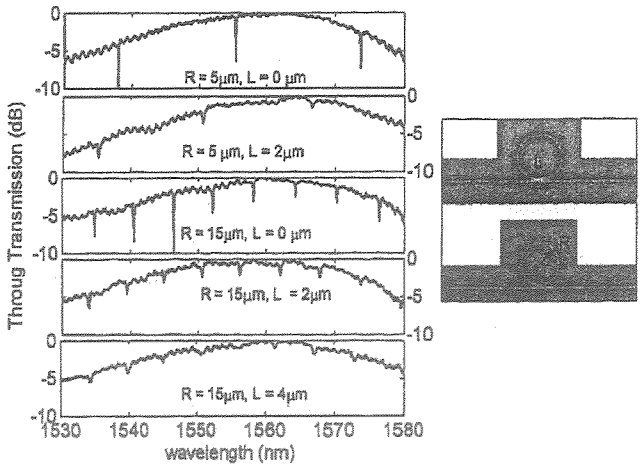

Fig. 8 The through output of various one-ring one-bus devices with different loss (radii, R) and coupling coefficients (racetrack lengths, L).

there is still some bowing in the spectra which is due to the grating envelope.

We note two remarkable features of these spectra. First

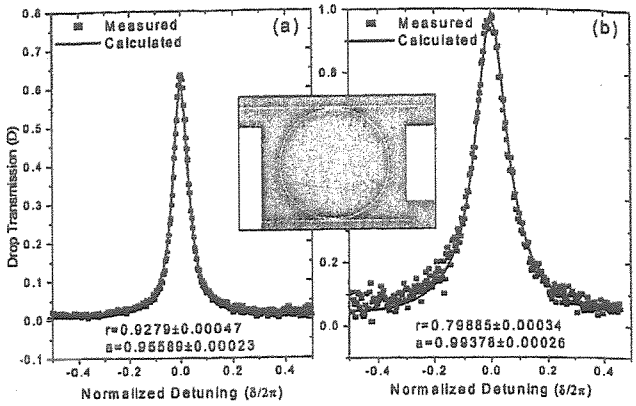

Fig. 9 The drop output of a single ring coupled with two bus waveguides (see inset) (a) without and (b) with oxide upper cladding. The ring radius is 15 μm and the race track length is 2 μm. The solid lines are theoretical fits.

is the relatively high contrast consistently shown by the different devices in both Sets A and B that have widely varying coupling coefficient and loss. By contrast, the transmission spectra of the one-ring-one-bus (1R1B) devices with varying radii and racetrack lengths that are fabricated on the same wafer show relatively small contrast, as shown in Fig. 8, which means that it is difficult for one-ring devices to even just achieve near critical coupling.

Second, it can be seen that the spectra of Fig. 6 closely resemble the simulated results shown in Fig. 2. Good theoretical fit with Eq. (5) can be achieved by varying the primary parameters r, r_1 and a_1. The best-fit values are $r_1 \sim 0.8$ and $r \sim 0.92$, and $a_1 \sim 0.96$ for set A, and $r_1 = r \sim 0.81$, and $a_1 \sim 0.993$ for set B. The r_1 and r values are in agreement with calculations based on the racetrack lengths given in Table 1, and are smaller for set B as expected. Similarly, a_1 is larger (i.e., loss is smaller) for set B due to the presence of the upper oxide cladding. Independent verification of the loss parameters can be made by studying the spectra of single-ring devices as well. Since the 1R1B case has poor contrast, we looked alternatively to the one-ring two-bus (1R2B) devices which were also fabricated in the same wafer. An example is shown in Fig. 9. The Drop spectra for the 1R2B device can be curve-fitted with the analytical formula $D = \frac{a(1-r^2)^2}{1+a^2r^4-2ar^2\cos\delta}$ [9], [10], yielding the values (a) $a = 0.95589 \pm 0.00023$ with $r = 0.9279 \pm 0.00047$ for set A, and (b) $a = 0.99378 \pm 0.00026$ and $r = 0.79885 \pm 0.00034$ for set B, which are quite close to the earlier values given above.

The detailed fit between theory and experiment is shown in Fig. 10 for the broad and narrow resonances of the γ=2 devices. The curve fit is quite good for Set A. From this data, we find that the finesse of the narrow resonance is about 76. For the 1R1B case, since it is difficult to measure the finesse, we simply calculate the finesse (F) under the critical coupling condition using the fitting parameter, i.e., $F = \pi r/(1 - r^2)$, where $r = 0.8$, which gives about 7. Alternatively, we may consider the 1R2B case, for which the finesse is measured to be 6.4. The finesse enhancement is thus about 10.8 over the 1R1B case, or 11.8 over the 1R2B

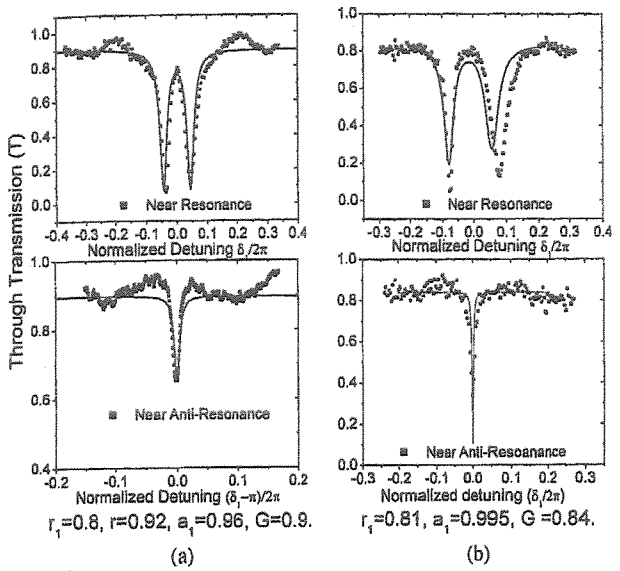

Fig. 10 The parameter extraction for $\gamma = 2$ devices (a) without and (b) with top oxide cladding.

case, both in fairly good agreement with Eq. (7), which gives a value of ~ 11.2 using the best fit values of a and r given above. Similarly, for set B the finesse of the narrow resonance is ~58 and the finesse for the 1R1B is ~7.4. Thus the enhancement is about 7.8, again quite close to the theoretical value of 8.9 given by Eq. (7).

4. Conclusion

We have theoretically and experimentally demonstrated that the two-ring system can exhibit interesting transmission properties when their sizes are different. Theory predicts and the experiment verifies that the transmission maintains relatively high contrast for devices with very different round-trip loss and coupling coefficient, unlike the one-ring one-bus case which has difficulty in showing critical coupling. Experimentally, the results are in a good agreement with theory for a range of γ values. The case of $\gamma = 2$, in particular, produced a narrow resonance dip, with the finesse enhancement proportional to the field enhancement factor in the second ring in agreement with theory. The extracted parameters are verified with independent curve-fitting of the results for one-ring devices coupled to two bus waveguides.

Acknowledgments

The author would like to thank Mr. Lee Chee Wei for oxide deposition.

References

[1] Q. Xu, S. Manipatruni, B. Schmidt, J. Shakya, and M. Lipson, "12.5 Gbit/s carrier-injection-based silicon micro-ring silicon modulators," Opt. Express, vol.15, pp.430–436, 2007.

[2] Q. Xu and M. Lipson, "All-optical logic based on silicon micro-ring resonators," Opt. Express, vol.15, pp.924–929, 2007.

[3] C.Y. Chao, W. Fung, and L.J. Guo, "Polymer microring resonator for biochemical sensing applications," IEEE J. Sel. Top. Quantum Electron., vol.12, pp.134–142, 2004.

[4] K. De Vos, I. Bartolozzi, E. Schacht, P. Bienstman, and R. Baets, "Silicon-on-insulator microring resonator for sensitive and label-free biosensing," Opt. Express, vol.15, pp.7610–7615, 2007.

[5] A. Yariv, "Critical coupling and its control in optical waveguide-ring resonator systems," IEEE Photonics Technol. Lett., vol.14, pp.483–485, 2002.

[6] J. Niehusmann, A. Vörckel, P.H. Bolivar, T. Wahlbrink, W. Henschel, and H. Kurz, "Ultrahigh-quality-factor silicon-on-insulator microring resonator," Opt. Lett., vol.29, pp.2861–2863, 2004.

[7] P. Dumon, W. Bogaerts, V. Wiaux, J. Wouters, S. Beckx, J.V. Campenhout, D. Taillert, B. Luyssaert, P. Bienstman, D.V. Thourhout, and R. Baets, "Low-loss SOI photonic wires and ring resonators fabricated with deep UV lithography," IEEE Photonics Technol. Lett., vol.16, pp.1328–1330, 2004.

[8] W. Bogaerts, R. Baets, P. Dumon, V. Wiaux, S. Beckx, D. Taillaert, B. Luyssaert, J. Van Campenhout, P. Bienstman, and D. Van Thourhout, "Nanophotonic waveguides in silicon-on-Insulator with CMOS technology," J. Lightwave Technol., vol.23, pp.401–412, 2005.

[9] Y.M. Landobasa, S. Darmawan, and M.K. Chin, "Matrix analysis of 2-D micro-resonator lattice optical filters," IEEE J. Quantum Electron., vol.41, pp.1410–1418, 2005.

[10] The fitting is performed using ORIGIN software.

Landobasa Y.M.A.L. Tobing was born in 1981. He received his B.Eng. and M.Sc. degrees in Electronic and Electrical Engineering from Nanyang Technological University, Singapore, in year 2003 and 2004 respectively. Currently he is pursuing his Ph.D. degree in the same university. His current research interests include photonic crystal and ring resonator arrays.

Pieter Dumon received the electrical engineering degree from Ghent University, Gent, Belgium, in 2002, where he is currently working toward the Ph.D. degree in electrical engineering. His research interests include the modeling, design, and fabrication of nanophotonic waveguides and structures for passive photonic integrated circuits.

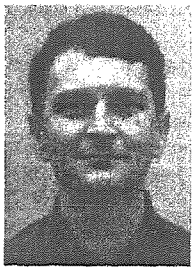

Roel Baets received the electrical engineering degree from Ghent University, Gent, Belgium, in 1980, the M.Sc. degree in electrical engineering from Stanford University, Stanford, CA, in 1981, and the Ph.D. degree from Ghent University in 1984. He joined the Department of Information Technology (INTEC) of Ghent University in 1981, and since 1989, he has been a Professor in the engineering faculty. He has mainly worked in the field of photonic components and has about 300 publications and conference papers. He currently leads the Photonics Group at the Ghent University Department of Information Technology (INTEC), which is an associated laboratory of the Interuniversity Microelectronics Center (IMEC), working on integrated photonic devices for optical communication, optical interconnect, and optical sensing.

Desmond C.S. Lim is member of technical staff in Singapore Defense Science Organization National Laboratories, and an adjunct assistant professor in Nanyang Technological University. He obtained the Ph.D. degree from the Massachusetts Institute of Technology in 2000. His main research interest is in microwave photonics and integrated optics.

Mee-Koy Chin is an associate professor of Electrical Engineering in Nanyang Technlogical University (NTU), Singapore. His research interests include integrated optics and nanophotonics. He received the B.S. degree from the Massachusetts Institute of Technology in 1986, and the Ph.D. from the University of California, San Diego in 1992. He joined NTU in 1993 where he founded the first Photonics Research Laboratory in Singapore. He then left in 1997 and spent several years in industry in the U.S. before re-joining NTU in 2003. He is the current chair of the IEEE Laser and Electro-optics Soceity Singapore Chapter.